ARMY RESEARCH LABORATORY

Microstructures of Mercury-Based Cuprate Thin Films

J.Z. Wu, S.H. Yun, Steven C. Tidrow and Donald W. Eckart

ARL-TR-937

January 1997

19970402 091

NOTICES

Disclaimers

REPORT DOCUMENTATION PAGE

1. AGENCY USE ONLY *(Leave blank)*	2. REPORT DATE January 1997	3. REPORT TYPE AND DATES COVERED Technical Report

4. TITLE AND SUBTITLE

MICROSTRUCTURES OF MERCURY-BASED CUPRATE THIN FILMS

5. FUNDING NUMBERS

6. AUTHOR(S)

J.Z. Wu,* S.H. Yun,* Steven C. Tidrow and Donald W. Eckart

7. PERFORMING ORGANIZATION NAMES(S) AND ADDRESS(ES)

US Army Research Laboratory (ARL)
Sensors and Electron Devices Directorate
ATTN: AMSRL-SE-EO
Fort Monmouth, NJ 07703-5601

8. PERFORMING ORGANIZATION REPORT NUMBER

ARL-TR-937

9. SPONSORING / MONITORING AGENCY NAME(S) AND ADDRESS(ES)

10. SPONSORING / MONITORING AGENCY REPORT NUMBER

11. SUPPLEMENTARY NOTES

*J.Z. Wu and S.H. Yun are with the University of Kansas, Department of Physics and Astronomy, Lawrence, KS 66045.

12a. DISTRIBUTION / AVAILABILITY STATEMENT

Approved for public release; distribution is unlimited.

12 b. DISTRIBUTION CODE

13. ABSTRACT *(Maximum 200 words)*

The microstructures of mercury-based cuprate thin films have been studied using a scanning electron microscope and an energy dispersive x-ray spectrometer. Besides rough surface, several types of defects including $HgCaO_2$ phase are identified on those films made using a slow temperature ramping Hg-vapor annealing process. By ramping the sample temperature rapidly to the annealing temperature, the surface morphology of the film is significantly improved and the impurity phases, especially the $HgCaO_2$ phase, are effectively reduced.

14. SUBJECT TERMS

High critical temperature superconductors; mercury-based superconductors; thin films; microstructure

15. NUMBER IF PAGES

13

16. PRICE CODE

17. SECURITY CLASSIFICATION OF REPORT Unclassified	18. SECURITY CLASSIFICATION OF THIS PAGE Unclassified	19. SECURITY CLASSIFICATION OF ABSTRACT Unclassified	20. LIMITATION OF ABSTRACT UL

CONTENTS

LIST OF FIGURES

MICROSTRUCTURES OF MERCURY-BASED CUPRATE THIN FILMS

INTRODUCTION

Development of high-quality Hg-based cuprate ($HgBa_2Ca_{n-1}Cu_nO_{2n+2+\delta}$, n=1-5) thin films is of primary importance for numerous electronic device applications because of their potential to be operated at temperatures above 120 K [1,2]. However, the high volatility and high toxicity of Hg and Hg-based compounds makes synthesis of such films extremely difficult. Considerable progress has been made recently which includes fabrication of c-axis oriented $HgBa_2Ca_1Cu_2O_{6+\delta}$ (Hg-1212) thin films using atomic-scale mixing of $HgO/Ba_2Ca_1Cu_2O_{6+\delta}$ precursors followed by Hg-vapor annealing [3] and fabrication of c-axis oriented Hg-1212 and $HgBa_2Ca_2Cu_3O_{8+\delta}$ (Hg-1223) thin films using fast temperature ramping Hg-vapor annealing (FTRA) of non-Hg-containing $Ba_2Ca_{n-1}Cu_nO_{2n+2+\delta}$ (n=2,3) precursor films [4,5]. Both of these processes are composed of two steps: deposition of either Hg-containing or Hg-free rare-earth copper precursor films and high temperature Hg-vapor annealing. Since the precursor films are amorphous and insulating, the Hg-based superconducting phases are formed during post Hg-vapor annealing when Hg is incorporated into the film through thermal diffusion. Since the film properties depend directly on the annealing process, important information on the growth mechanism (which is not well understood due to the volatility of Hg) of the Hg-based cuprate thin films is contained in microstructure and surface morphology data. Therefore, we have recently conducted a systematic study on the microstructures and surface morphology of the Hg-1212 and Hg-1223 thin films using scanning electron microscopy (SEM) and energy dispersive x-ray spectroscopy (EDS) techniques. In this article, we present the experimental results of the investigation.

SAMPLE PREPARATION

The details of sample preparation have been reported previously [4,5]. Briefly, the precursor $Ba_2Ca_2Cu_3O_x$ films are radio-frequency sputtered from a $Ba_2Ca_2Cu_3O_x$ target onto (100)-oriented $SrTiO_3$ or $LaAlO_3$ substrates at room temperature in 0.05 Torr pure Argon. The deposition chamber is pumped down to 10^{-6} Torr and flushed with pure Ar gas before deposition begins. The target is presputtered for half an hour each time before the film is deposited in order to remove the target surface layer. The controlled thicknesses of the precursor films range from 0.2 to 0.8 μm as calibrated using the cross-sectional thickness obtained from SEM. The films used for SEM/EDS study in this work are all around 0.35 μm. After sealing the film in a precleaned and evacuated quartz tube together with pellets of unreacted $HgBa_2Ca_2Cu_3O_x$ and precursor $Ba_2Ca_2Cu_3O_x$, the precursor films are annealed at high temperatures for varying periods. Two different annealing processes are used: conventional slow temperature ramping Hg-vapor annealing (STRA) [3,6] in which the sample assembly

temperature is slowly increased at a rate of 2.5 °C/min.; and FTRA [5] in which the sample assembly temperature is rapidly increased (>10 °C/min.) to the annealing temperature. For some cases of FTRA the sample assembly is inserted into a preheated furnace directly, thus, the heating period is estimated to be less than one minute. In both STRA and FTRA processes, the sample assembly is held at the annealing temperature (790-860 °C) for 15-60 minutes and then cooled slowly (2.5-5 °C/min.) to room temperature.

EXPERIMENTAL RESULTS

Fig. 1 shows SEM pictures of the typical surface morphology of Hg-1223 films made using the STRA process. These films were annealed for 30 min. at 800 °C. In Fig. 1(a), several different types of phases can be identified using the EDS technique with a focused electron beam. The large size grains are superconductor grains which have the same composition as that expected for the stoichiometric Hg-1223 phase. Square and hexagonal shape blocks are a Ba and Cu rich phase which has a composition ratio of Ba:Cu of 2:1 and very little trace of Hg and Ca. The small irregular shape blocks are a Ca and Hg rich phase as confirmed by EDS and the bright image in the backscattering micrograph of the film as shown in Fig. 1(b). EDS analysis on the bright spots indicates that these irregular shaped small blocks have a composition of $HgCaO_2$, a major impurity phase formed during Hg-vapor STRA of the Hg-based superconductors. Hg-compounds such as HgO are extremely volatile. For example, HgO which was used in this experiment decomposes at around 500 °C and Hg^{+2} starts to react with the precursor as Hg diffuses through the sample surface. Since the formation of Hg-based cuprate superconducting phases requires annealing temperatures around 800 °C, the formation of $HgCaO_2$ can dominate during the heating process from 500-800 °C. During Hg-vapor STRA processing of films, the precursor sample spends an exceedingly long period of time (roughly 2 hours) in the temperature range 500-800 °C where formation of $HgCaO_2$ can occur. Even though the STRA process has been used successfully for fabrication of bulk Hg-based superconductors, the phase diagram may not be favorable and/or the kinetics for formation of $HgCaO_2$ may be sluggish such that only a small volume fraction of a large bulk sample has the $HgCaO_2$ impurity phase. On the other hand, the same STRA processing of a thin film can result in a relatively large volume fraction of the $HgCaO_2$ impurity phase. $HgCaO_2$ seriously degrades the superconducting properties of the film because the volume portion of the superconducting phase will be significantly reduced. Moreover, as shown in Fig. 1(a), a relatively rough surface morphology has been observed in most films made using the STRA process. The surface roughness over a 10 µm length ranges from 30-90 % of the film thickness from a cross-section SEM study. Moreover, holes are visible in many of these films and EDS analysis over the hole area discerns mostly substrate signals indicating that these holes are almost through the film. Even though these films are c-axis oriented as suggested by the x-ray diffraction pattern [7], poor alignment of the film with respect to the substrate has been demonstrated using an ion beam channeling experiment.

Most Hg-based superconducting thin films made using the STRA process also have a poor film/substrate interface structure as confirmed using Auger and Rutherford backscattering (RBS) analysis which reveal serious Ba diffusion into the substrates. The range of Ba diffusion, typically a few μm, increases with the Hg-vapor annealing time and temperature. When the total high temperature processing time is effectively reduced in the FTRA process, the Ba diffusion range is also reduced which results in a better film/substrate interface. The details of the Auger and RBS study will be published elsewhere. In particular, when the annealing temperature is higher than 800 °C in the STRA process, an island type of growth of the superconducting phase is observed as shown in Fig. 2. The brighter islands in the backscattering micrograph (right half) are found to be stoichiometric Hg-1223 phase while the darker portion connecting these islands is an Hg-deficient and Ca-deficient Hg-1223 phase with poor superconducting properties. This is easily understood due to formation of the $HgCaO_2$ impurity phase. Observation of the relatively large volume fraction of the $HgCaO_2$ impurity in the film is consistent with the low zero-resistance T_c and low critical current density (J_c) of these samples [7].
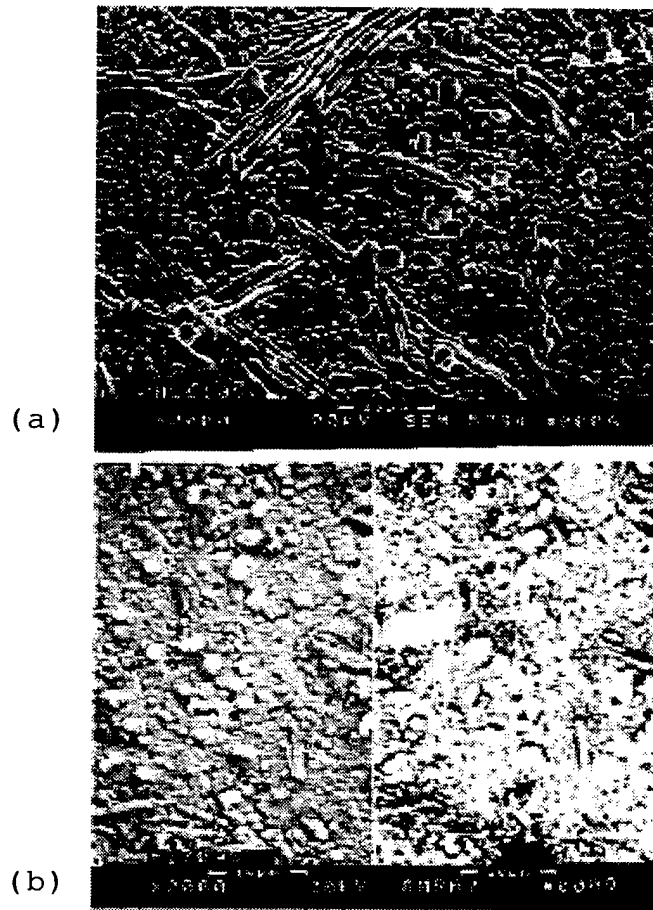
(a)

(b)

Figure 1. SEM pictures of Hg-1223 films fabricated at 800 °C using the STRA process. The upper was taken using a secondary electron detector and lower is a split screen of secondary (left) and backscattered SEM. Both pictures have a magnification of 2000.
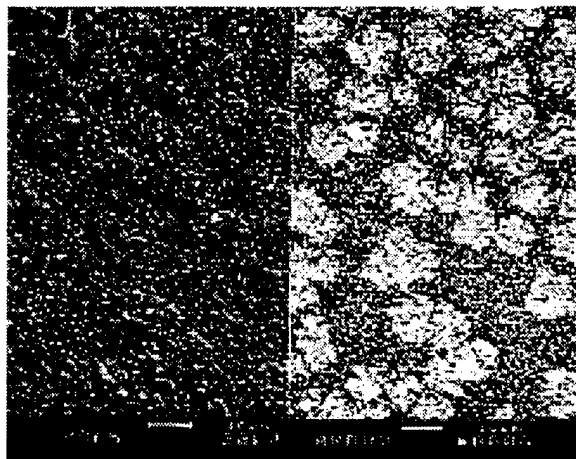
Figure 2. SEM picture of an Hg-1223 film fabricated at 820 °C using the STRA process.

Both superconducting phase purity and surface morphology of Hg-based cuprate thin films can be significantly improved by using the FTRA process. In the FTRA process, the heating period is reduced from 5-6 hours to typically 1-15 minutes. Fig 3 shows a typical SEM of the surface morphology for an Hg-1223 film made using the FTRA (50 °C/min.) process. The annealing period, temperature and the cooling process used for this sample are similar to that for the sample shown in Fig. 1. As shown in Fig. 3, only a few bright spots are visible indicating that the amount of $HgCaO_2$ is greatly reduced when the FTRA process is adopted. This is consistent with the x-ray diffraction pattern of the same sample where little trace of $HgCaO_2$ was detected. The surface roughness of the film has been reduced to 20-35 % of the film thickness over a 10 μm range. The well connected network of superconducting phase as seen in Fig. 3 results in a high zero-resistance T_c between 125-130 K and high J_c's, for example, up to 3×10^6 A/cm^2 at 77 K and zero field.
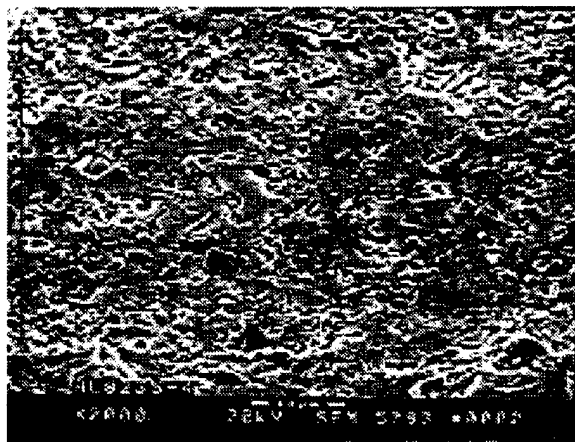

Figure 3. SEM picture of an Hg-1223 film fabricated using the FTRA process.

Even using the FTRA process, the surface morphology of the Hg-based cuprate thin films is found to be sensitive to the partial pressure of the Hg-vapor which is controlled by the mass ratio between the unreacted stoichiometric pellet and the non-Hg-contain rare-earth cuprate pellet and the

4

ratio between the total mass of two pellets and the volume of the quartz tube. Fig. 4 shows a comparison of two Hg-1223 films made using the same FTRA process with nonstoichiometric unreacted bulk pellets. Fig. 4(a) corresponds to a sample annealed using 15 % (wt) more HgO in the pellet while Fig. 4(b) corresponds to a sample annealed using 15 % (wt) less HgO in the pellet. In conjunction with Fig. 3 in which the film was annealed using a stoichiometric pellet, it is observed that the surface of the film is smoother when the Hg-content in the pellet is slightly below stoichiometry. It is interesting to point out that the superconducting properties such as T_c and J_c of all three films are comparable.
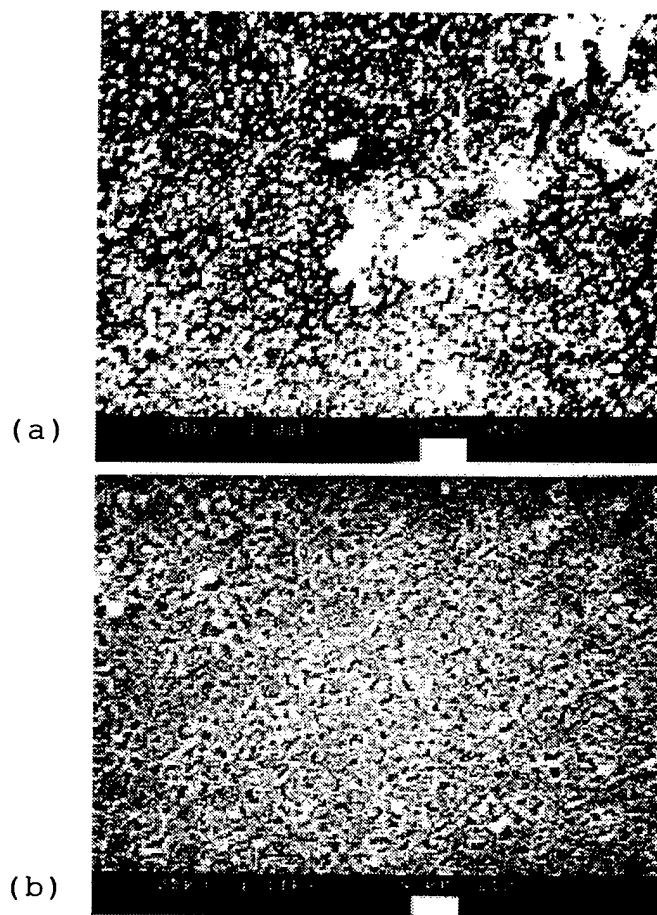

(a)

(b)

Figure 4. Comparison of surface morphology of Hg-1223 thin films made with 15 % (wt) more (upper) and 15 % (wt) less Hg in the unreacted stoichiometric pellet.

The detrimental effects of moisture and CO_2 on the FTRA processing of the precursor films are less significant than for STRA processing. However, films with degraded superconducting properties do occur and are a serious concern since the mechanism of contamination is not clearly understood. As shown in Fig. 5, two types of "poor" quality films have been observed and may result from contamination of moisture and CO_2 from the air. One has a light grey color [Fig. 5(a)] or can be even transparent and is completely insulating after Hg-vapor annealing. The other is initially superconducting after Hg-vapor annealing and gradually degrades (within 30 min. to 1-2 hours) if thermal cycling is applied. In this case, a color change of the film from black to transparent is visible

during the degradation. Cracks in the film are observed in the SEM picture as shown in Fig. 5(b). It is observed in both of these "poor" quality films that Ca-content is only one third to half of the correct stoichiometry. Further investigation into this issue is underway in order to understand the mechanism for contamination and film degradation.
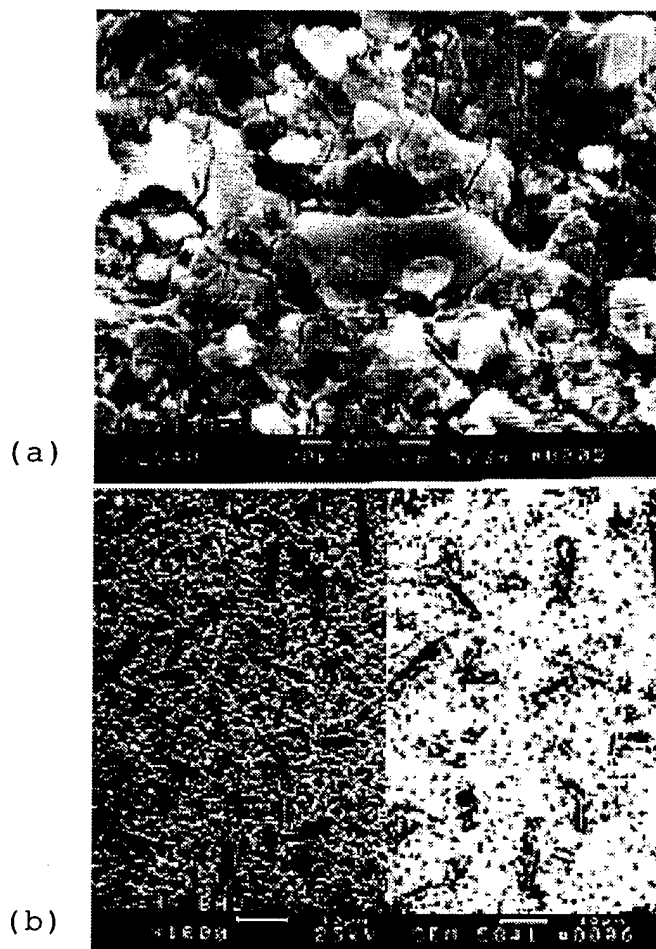

(a)

(b)

Figure 5. Surface morphology of contaminated Hg-1223 thin films. (Upper) "Poor" film immediately after the annealing and (lower) degraded film after one thermal cycle.

In conclusion, the surface morphology of Hg-1223 thin films can be significantly improved using FTRA processing. Impurity phases, especially the $HgCaO_2$ are effectively suppressed using FTRA processing. FTRA processing of Hg-based superconductors results in high quality superconducting Hg-based cuprate thin films that are useful for many applications.

ACKNOWLEDGEMENTS

6

REFERENCES

[1] S. N. Putilin, E. V. Antipov, O. Chmaissem, and M. Marezio, Nature **362**, 226 (1993).

[2] A. Schilling, M. Cantoni, J. D. Guo, and H. R. Ott, Nature **363**, 56 (1993).

[3] C. C. Tsuei, A. Gupta, G. Trafas, and D. Mitzi, Science **263**, 1259 (1994).

[4] S. H. Yun and J. Z. Wu, Appl. Phys. Lett. **68**, 862 (1996).

[5] J. Z. Wu, S. H. Yun, S.C. Tidrow and D.W. Eckart, Appl. Phys. Lett. **68**, 2565 (1996).

[6] Y. Q. Wang, R. L. Meng, Y. Y. Sun, Z. J. Huang, K. Ross and C. W. Chu, Appl. Phys. Lett. **63**, 3084 (1993).

[7] S. H. Yun, J. Z. Wu, B. W. Kang, A. N. Ray, A. Gapud, Y. Yang, R. Farr, G. F. Sun, S. H. Yoo, Y. Xin, and W. S. He, Appl. Phys. Lett. **67**, 2866 (1995).

ARMY RESEARCH LABORATORY   Jan 1997
SENSORS AND ELECTRON DEVICES DIRECTORATE   Page 1 of 2
MANDATORY DISTRIBUTION LIST

Defense Technical Information Center*
ATTN: DTIC-OCC
8725 John J. Kingman Rd, STE 0944
Fort Belvoir, VA 22060-6218
(*Note: Two DTIC copies will be sent
from STINFO office, Ft Monmouth, NJ)

Director
US Army Material Systems Analysis Actv
ATTN: DRXSY-MP
(1) Aberdeen Proving Ground, MD 21005

Commander, AMC
ATTN: AMCDE-SC
5001 Eisenhower Ave.
(1) Alexandria, VA 22333-0001

Director
Army Research Laboratory
ATTN: AMSRL-D (John W. Lyons)
2800 Powder Mill Road
(1) Adelphi, MD 20783-1197

Director
Army Research Laboratory
ATTN: AMSRL-DD (COL Thomas A. Dunn)
2800 Powder Mill Road
(1) Adelphi, MD 20783-1197

Director
Army Research Laboratory
2800 Powder Mill Road
Adelphi, MD 20783-1197
(1) AMSRL-OP-SD-TA (ARL Records Mgt)
(1) AMSRL-OP-SD-TL (ARL Tech Library)
(1) AMSRL-OP-SD-TP (ARL Tech Publ Br)

Deputy Director
Army Research Laboratory
Sensors & Electron Devices Directorate
Fort Monmouth, NJ 07703-5601
(1) AMSRL-SE
(1) AMSRL-SE-C (V. Rosati)
(1) AMSRL-SE-C (M. Hayes)
(1) AMSRL-OP-FM-RM
(22) Originating Office

Advisory Group on Electron Devices
ATTN: Documents
Crystal Square 4
1745 Jefferson Davis Highway, Suite 500
(2) Arlington, VA 22202

Commander, CECOM
R&D Technical Library
Fort Monmouth, NJ 07703-5703
(1) AMSEL-IM-BM-I-L-R (Tech Library)
(3) AMSEL-IM-BM-I-L-R (STINFO Ofc)

Deputy for Science & Technology
Office, Asst Sec Army (R&D)
(1)   Washington, DC 20310

Cdr, Marine Corps Liaison Office
ATTN: AMSEL-LN-MC
(1)   Fort Monmouth, NJ 07703-5033

HQDA (SARDA-TR)
Dr. Richard Chait
(1)   Washington, DC 20310

Director
Naval Research Laboratory
ATTN: Code 2627
(1)   Washington, DC 20375-5000

USAF Rome Laboratory
Technical Library, FL2810
ATTN: Documents Library
Corridor W, STE 262, RL/SUL
26 Electronics Parkway, Bldg 106
Griffiss Air Force Base
(1)   NY 13441-4514

Dir, ARL Battlefield
Environment Directorate
ATTN: AMSRL-BE
White Sands Missile Range
(1)   NM 88002-5501

Dir, ARL Sensors, Signatures,
Signal & Information Processing
Directorate (S3I)
ATTN: AMSRL-SS
2800 Powder Mill Road
(1)   Adelphi, MD 20783-1197

Dir, CECOM Night Vision/
Electronic Sensors Directorate
ATTN: AMSEL-RD-NV-D
(1)   Fort Belvoir, VA 22060-5806

Dir, CECOM Intelligence and
Electronic Warfare Directorate
ATTN: AMSEL-RD-IEW-D
Vint Hill Farms Station
(1)   Warrenton, VA 22186-5100